C. R. Physique 3 (2002) 251–272

Solides, fluides : structure/*Solids, fluids: structure*
(Atomes, molécules/*Atoms, molecules*)

DOSSIER

AGRÉGATS COMME PRÉCURSEURS DES NANO-OBJETS
CLUSTERS AS PRECURSORS OF NANO-OBJECTS

Met-Cars: a unique class of molecular clusters

Brian D. Leskiw, A. Welford Castleman Jr.

Departments of Chemistry and Physics, The Pennsylvania State University, University Park, PA 16802, USA

Received 26 October 2001; accepted 21 December 2001

Note presented by Guy Laval.

Abstract Currently there is extensive interest in systems of finite size as they often give rise to unique properties that differ from those of an extended solid or the individual molecular constituents of which they are comprised. Particularly interesting are systems whose composition can be selectively chosen, and ones whose individual characteristics may be retained, thus allowing them to serve as the building blocks for nanostructured/cluster-assembled materials. In 1992 we discovered a new class of molecular clusters termed metallocarbohedrenes, or Met-Cars for short, which involve bonding between early transition metals and carbon with a stoichiometry of M_8C_{12}. Calculations, as well as recent experimental findings, suggest that these species exhibit considerable free electron behavior which becomes manifested through observations of changing electronic energy levels with the nature of the metal. Indications that it is possible to produce Met-Cars with various endohedral atoms, as well as the finding that other metals and non-metal atoms may also be substituted in the cage lattice, suggest that these cluster materials are valuable in the context of unraveling the properties of condensed matter of finite size. This also opens an avenue for exploring the prospect that they may provide building blocks for new materials. Their discovery, formation, and ionization dynamics are reviewed herein. ***To cite this article: B.D. Leskiw, A.W. Castleman, C. R. Physique 3 (2002) 251–272.*** © 2002 Académie des sciences/Éditions scientifiques et médicales Elsevier SAS

Met-Cars / delayed ionization / cluster / ionization potential / electron relaxation dynamics

Met-Cars : une classe unique d'agrégats moléculaires

Résumé L'intérêt primordial des systèmes de taille finie réside dans les propriétés spécifiques qu'ils présentent, qui diffèrent de celles de leurs constituants et de celles du solide correspondant. Ces systèmes, dont on peut choisir la composition et pour lesquels les propriétés des constituants individuels sont préservées, apparaissent particulièrement séduisant car ils sont utilisables comme briques élémentaires pour construire des matériaux nanostructurés. En 1992, nous avons découvert une nouvelle catégorie d'agrégats moléculaires, les « Met-Cars », impliquant une liaison carbone-M où M est un atome des premiers métaux de transition, avec une stoechiométrie M_8C_{12}. Les calculs ainsi que les données expérimentales récentes suggèrent pour ces espèces un comportement de type à électrons libres, ce que l'on peut montrer clairement en changeant la nature du métal. La possibilité de produire des « Met-Cars » avec différents atomes internes et différents atomes, métalliques ou non, pour la cage, montre bien que ces édifices sont précieux pour appréhender les propriétés de la matière condensée de taille finie. Ceci ouvre aussi une large voie d'exploration quant

E-mail addresses: bdl121@psu.edu (B.D. Leskiw); awc@psu.edu (A.W. Castleman).

S1631-0705(02)01319-1/FLA

à leur utilisation comme briques élémentaires pour élaborer de nouveaux matériaux. Leur découverte, leur production et la dynamique de leur ionisation, sont présentées. ***Pour citer cet article : B.D. Leskiw, A.W. Castleman, C. R. Physique 3 (2002) 251–272.***

Met-Cars / ionisation retardée / agrégat / potentiel d'ionisation / dynamique de relaxation des électrons

1. Introduction

Systems of finite size often display unique properties, and elucidating the differences compared to those of extended systems provides a challenge of considerable current scientific interest. Systems, whose composition can be selectively altered, offer the prospect of forming materials of desired physical, chemical, and electronic behavior. If such matter can be assembled in a manner where each entity retains its individual characteristics, there is an opportunity to produce new nanostructured materials with tailored properties. From an applications point of view, there is currently extensive interest in the prospect of producing new materials, both stable and metastable, comprised of carbon, nitrogen, and silicon bound in various combinations to transition metals. The growing interest in these compounds has arisen due to the fact that many are found to have novel properties which make them good potential candidates as new electronic materials including use as semiconductors, implants for quantum well and quantum dot devices, and of possible value in the construction of solar cells, photovoltaic devices, and optical switches. The quantum effects that materials of finite size and dimension often show, add to the interest in the special properties.

In terms of developing a more extensive fundamental understanding of factors governing the properties of finite size systems, studying materials comprised of clusters is particularly revealing since they provide the opportunity, for example, to investigate when discrete molecular properties begin to coalesce and display the collective behavior characteristic of solids (e.g., band structure). Describing such phenomena requires the use of concepts which bridge atomic and molecular physics on the one hand, with the field of condensed matter science on the other. Small systems often display optical absorption features attributable to quantum confinement and at higher energies the onset of giant dipole collective resonances. Systems of limited size also sometimes show behavior that can display semiconductor to metallic-like characteristics.

Other important related scientific topics, which can be addressed through cluster research, involve issues related to the field of molecular dynamics, such as whether large molecules facilely ionize upon optical excitation, undergo autoionization, or alternatively decay through electronic to vibrational relaxation and ultimately predissociate prior to ionization. A related issue is determining the nature of the phenomenon of delayed ionization in small systems, which has thermionic emission as its bulk phase analogue, and also ascertaining how the electronic states of mixed transition metal containing clusters couple in terms of their ionization characteristics. Of significance are questions addressing whether there is a behavioral difference attributable to the time domain of the ionization source, i.e., nanosecond versus femtosecond electromagnetic radiation. Answering these questions for systems comprised of metal compound clusters will have a significant impact on understanding the properties of new materials, and the prospects of using clusters to tailor the design of new nanoscale materials of desired properties.

2. The discovery of Met-Cars: a new class of molecular clusters

During the course of undertaking detailed studies of dehydrogenation reactions of hydrocarbons induced by titanium ions, atoms, and clusters [1–5], we discovered the formation of an unusually abundant and stable cationic species having a molecular weight of 528 amu, which we thereafter established contains eight titanium atoms and twelve carbons [6]. Subsequent work revealed the existence of the neutral molecular cluster, its anion analogue, the stability of other transition metal–carbon complexes of identical

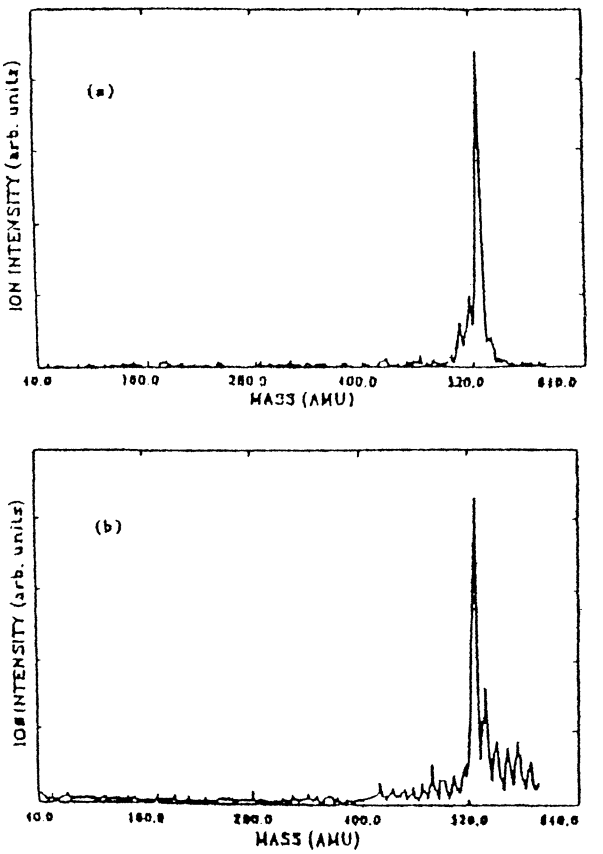

Figure 1. (a) Mass distribution of $Ti_mC_n^+$ clusters generated from the reactions of titanium with CH_4. (b) Mass distribution of $Ti_mC_n^+$ clusters generated from the reactions of titanium with C_2H_2. Note the predominant peak corresponding to $Ti_8C_{12}^+$.

stoichiometry, and thereafter a general class of caged molecular clusters [7–19]. Finally, our studies laid the foundation for a methodology useful for producing clusters comprised of transition metal carbides, nitrides, silicides, and oxides [10,11,20,21].

The experimental method employed in the work leading to the discovery was based on tandem mass spectrometry, described elsewhere [22]. The first Met-Car molecular cluster ion was generated through reactions of titanium with vapors of a variety of small hydrocarbon molecules, utilizing a laser-based plasma reactor. Fig. 1 shows a mass distribution of titanium carbide clusters formed through the reactions of titanium with two different hydrocarbon molecules; Fig. 1a was obtained with methane, and Fig. 1b with acetylene. As seen from Fig. 1, a peak at 528 amu is dominant in both mass spectra and no other prominent peaks are observable in the mass range below 1200 amu. Reactions with ethylene, benzene, and propylene, also generated similar cluster distributions, as did ones conducted with rods of Ti and graphitic powders [23].

Following these observations, we first undertook a series of studies with hydrocarbons of varying isotopic composition in order to definitively establish the identity of this unusually stable species. Isotope labeling experiments with deuterated organic compounds did not display any shift in mass, showing that the clusters corresponding to the peak at 528 amu did not contain any hydrogen atoms. 13C labeling experiments established that the cluster accommodated exactly twelve carbon atoms; see Fig. 2. Subsequent high-resolution isotope distribution pattern analyses supported the presence of eight Ti atoms, leading to the assignment of $Ti_8C_{12}^+$. Based on preliminary findings we suggested that this species (as well as its corresponding neutral molecule discovered later) might have a pentagonal dodecahedron structure. In this

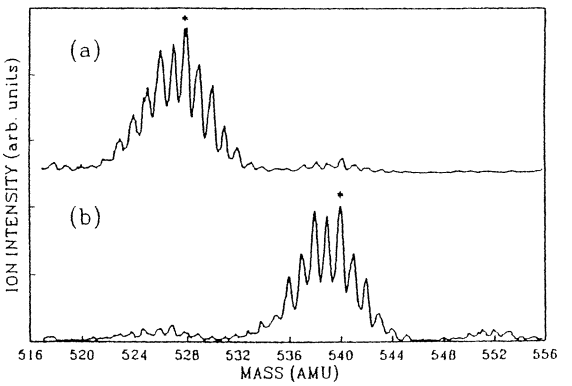

Figure 2. Mass spectra of $Ti_8C_{12}^+$ clusters generated from reactions of titanium with hydrocarbons containing different carbon isotopes; (a) $^{12}CH_4$, (b) $^{13}CH_4$. The subpeaks labeled * correspond to the molecule which contains the same number of ^{48}Ti and carbon atoms, but different carbon isotopes. Note the shift of the subpeak labeled * is 12 amu from (a) to (b).

arrangement, the Ti atoms would occupy eight unique positions that are identically coordinated and would thus contain twelve pentagonal rings consisting of two titanium atoms and three carbons. The initially proposed structure was based on titration experiments showing a smooth uptake of eight bonded ligands and subsequently implied that each of the titanium atoms were bonded to three carbon atoms through Ti–C bonds, and that each of the carbons were also bound to its adjacent carbon through a double bond. These Ti–C and C=C bonds connect all atoms together and form the network of the dodecahedral titanium-carbohedrene [24–32]. Variously bonded structures in addition to the pentagonal dodecahedron have been considered theoretically [33–42], and more recent experiments and theory tend to support a T_d structure [43,44] rather than one of the originally proposed T_h symmetry [6].

Later studies also revealed that it was possible to assemble Met-Cars of binary composition among the early transition metals such as Zr and Hf, as well as with some other atoms which do not form the pure Met-Car species, i.e., Y, Ta, W, and Si [45–47].

3. Cluster stability: CID, metastability and photodissociation

In order to provide insight on the extent of stability of Met-Car clusters, we also investigated their metastable decay using reflectron time-of-flight mass spectrometry [48,49], and collision-induced dissociation (CID) [50]. The metastable experiments reveal that Ti_8C_{12} loses Ti upon evaporative dissociation; alternatively, Ti_8C_{14} was observed to preferentially lose C_2 units. Findings also show that many single metal and carbon loss channels are active during the growth mechanism of Met-Car clusters [48,49] and an example of the stability of $Ti_8C_{12}^+$ over titanium carbides is illustrated in Fig. 3. The CID experiments also displayed a dominant Ti loss channel from the Met-Car, in general agreement with photodissociation experiments of Pilgrim and Duncan [51] made at 532 nm and more recent ones by May and Castleman [56]; a bond energy of $\leqslant 9$ eV for Ti loss was derived from our CID study. Similar metastable results were obtained for V_8C_{12} and Nb_8C_{12} [48].

In other related studies in our laboratory, neutral titanium-, niobium-, and zirconium-carbide clusters were studied by mass spectrometry, following laser photoionization, to address the question whether neutral Met-Cars are really stable. In order to support our earlier evidence for stable *neutral* Met-Cars, we recently conducted a thorough investigation on cluster source conditions during Met-Car formation. By simply varying the vaporization laser power, i.e., changing the relative concentrations of Ti and C atoms in the plasma, significant differences can be readily observed in the mass distribution; namely, either a dominant production of cubic carbides or Met-Car clusters [52]. Evidently, when the vaporization laser power is low, the plasma is not yet energetic enough to affect an efficient dehydrogenation process and thus not many pure carbon species are available for the formation of the metal–dicarbon (MC_2) units implicated in Met-Car formation. Reactions under these conditions typically terminate with the clusters either in a rock–salt structure when the beam is dominated by MC species, or a random assembly of carbon, titanium,

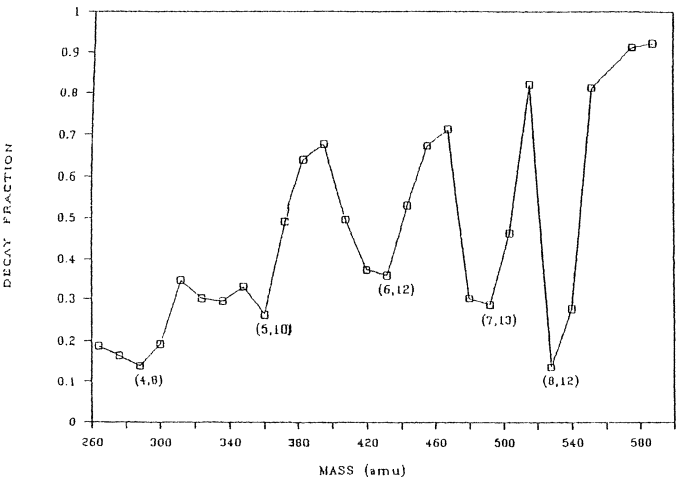

Figure 3. Measured decay fractions of $Ti_mC_n^+$. Local minima at (4,8), (5,10), (6,12), (7,13), and (8,12) are noticeable.

and perhaps some hydrogen atoms remaining attached when these species are only of minor composition. When the laser power is high, however, more pure carbon species are thus available for MC_2 development, and the clusters preferentially form Met-Cars. Theoretical calculations addressing the affects of the relative concentration of Ti and C atoms in the plasma, yielding carbides over Met-Car clusters, were also predicted by Reddy and Khanna [30]. Investigations of the niobium-, and zirconium–carbon systems, under differing vaporization laser power conditions, also gave further evidence in support of the proposed mechanism [52].

Interestingly, our experiments have revealed that neutral titanium Met-Cars are quite dominant under cluster source conditions where the vaporization laser power for cluster formation is very high. We also established that the photoabsorption, which eventually leads to photoionization, does not induce a significant amount of fragmentation under the ionization conditions. Moreover, studies discussed later conclusively show that neutral Met-Car clusters, containing bound ligands, can be produced prior to the ionization step that leads to detection thus eliminating the possibility that Met-Car clusters originate via the dissociation of larger metal–carbon species.

In order to investigate the stability of various members of the Met-Car cluster family, studies addressing the photofragmentation of the corresponding cluster ions were employed. Pilgrim et al. performed many studies on the single metal systems (see Table 1), and also provided results on some larger carbide clusters having a cubic-like structure [51,53–55]. Subsequently, we undertook a study to determine how the photofragmentation of several members of the binary metal Met-Car cluster family compares to previously reported results for the single metal Met-Cars, and also to determine whether or not there is a preference as to which metal in a binary metal Met-Car is lost first [56].

Three clusters systems were chosen for study to ultimately determine the effect of the overall electron count on the stability of the binary Met-Car cluster: Ti_7YC_{12}, Ti_7ZrC_{12}, and Ti_7NbC_{12}. The Ti_7ZrC_{12} cluster is isoelectronic to the initially discovered Ti_8C_{12}, while Ti_7YC_{12} contains one less metal electron, and Ti_7NbC_{12} contains one more. Preliminary electronic calculations carried out in our laboratory have suggested that the substitution of a yttrium atom into the Met-Car structure destabilizes the structure, while the substitution of a niobium atom contributes to a greater stability. These same results show that there is not an appreciable change in the stability of the cluster upon substitution of a zirconium atom for one of the titanium atoms. By comparing the resulting photofragments for each of the above clusters, any differences in the bonding sites between the different metals may be discerned. A typical dissociation scan for the $Ti_7YC_{12}^+$ cluster is shown in Fig. 4, and in this series of spectra, each successive photofragment is identified by the mass lost from the initial parent cluster [56].

As can be seen in Table 2, each of the three binary Met-Cars listed above are found to photodissociate through the successive losses of titanium atoms. While these results do not show a dependence of

Table 1. Summary of single metal containing Met-Car photodissociation as reported by May et al. [56] and Pilgrim et al. [51,53–55]. Each loss is denoted by the neutral fragment lost from the preceding parent. An X indicates that the previous parent is undetermined and the analysis and notation in the table assumes a stepwise fragmentation mechanism, although the exact mechanism remains experimentally unproven.

	$Ti_8C_{12}^+$	$Zr_8C_{12}^+$	$Cr_8C_{12}^+$	$Fe_8C_{12}^+$	$Mo_8C_{12}^+$
7/12	M	M	M	M	
7/10					MC_2
6/12	M		M	M	
6/10		MC_2			
6/9					M_2C_3
5/12	M		M	M	
5/8		MC_2			
5/7					M_2C_3, MC_2
4/12			M	M	
4/6		MC_2			M_2C_3
3/12			M	M	
2/12			M	M	
3/2			X	X	
2/2			X	X	
1/0	X	X	X	X	X

Table 2. Summary of photodissociative losses for $Ti_7YC_{12}^+$, $Ti_7ZrC_{12}^+$, and $Ti_7NbC_{12}^+$. An * indicates a loss channel observed under a separate study, but not for this particular parent cluster. Note that a loss channel for neither the carbon nor the metal was observed.

	$Ti_7YC_{12}^+$	$Ti_7ZrC_{12}^+$	$Ti_7NbC_{12}^+$
$Ti_7MC_{11}^+$			
$Ti_7MC_{10}^+$			
$Ti_7MC_9^+$			
$Ti_6MC_{12}^+$	Ti	Ti	Ti
$Ti_6MC_{11}^+$			
$Ti_6MC_{10}^+$			
$Ti_6MC_9^+$			
$Ti_7C_{12}^+$			
$Ti_5MC_{12}^+$	Ti	Ti	Ti
$Ti_7C_{11}^+$			
$Ti_4MC_{12}^+$	Ti	*	*

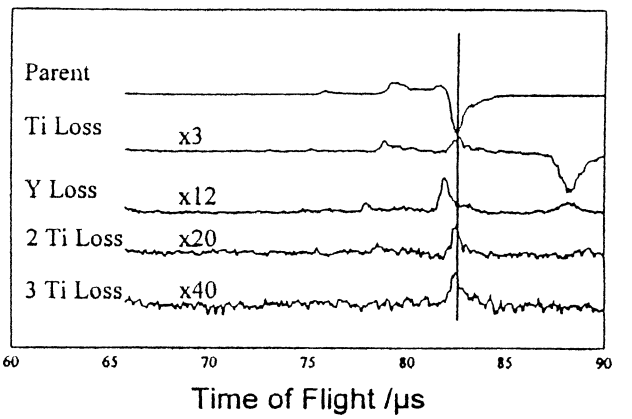

Figure 4. The dissociation scan showing all observed fragment channels of $Ti_7YC_{12}^+$. Note the absence of the Y loss channel and the presence of a channel corresponding to the loss of three Ti atoms. Relative ion intensity multiplication factors are shown for each trace.

the photofragment on the substituted metal, this may be merely an indication that the titanium loss is simply statistically more feasible because of the 7 : 1 ratio of Ti to the substituted metal in the clusters investigated [56]. However, with each successive loss, this ratio moves closer to unity, and there is no experimental indication of a loss channel involving the substituted metal. These results have yet to be extended to the more highly substituted members of these binary metallocarbohedrene families.

4. Growth of larger metal–carbon clusters

Following the analysis of single and binary metal Met-Cars, investigations of larger cluster systems were undertaken [9,57]. Interestingly, these studies revealed a unique structural growth pattern found in the system of Zr_mC_n, i.e., the formation of structures that do not follow the typical building pattern characteristic of cubic carbides. Careful examination of the experimental evidence showed that the first cage closes at Zr_8C_{12} but, surprisingly, subsequent cluster growth does not lead to the enlargement of the cage size as it usually does in the case of pure carbon clusters and water clusters, for example. Rather, multi-unit structures are developed corresponding to the compositions: $Zr_{13}C_{22}$ and $Zr_{14}C_{21}$, another at $Zr_{18}C_{29}$, and yet another at $Zr_{22}C_{35}$. Study of the niobium system revealed similar findings. This unique growth pattern distinguishes this class of metallocarbohedrenes from the regular doped fullerenes.

It is instructive to compare and contrast these findings with other metal–carbon systems. For example, those comprised of the single elements W, Co, and Ta do not assemble into the Met-Car structure, although they can become incorporated into the Met-Car through replacing a limited number of the main metal constituents. An interesting contrast to the Met-Car growth is provided by considering the tantalum-carbon system which builds through the formation of cubic-like clusters [8]. The observed magic numbers at (14,13), (18,18), (24,24), (32,32), (40,40), and (50,50) are consistent with cubic structures [9] which have closed packings of $3 \times 3 \times 3$, $3 \times 3 \times 4$, $3 \times 4 \times 4$, $4 \times 4 \times 4$, $4 \times 4 \times 5$, and $4 \times 5 \times 5$, in direct contrast to the magic number pattern of the Met-Cars [8,57]. Similar findings have also arisen from our studies of the titanium nitride system [21]; see Fig. 5. The failure to observe similar patterns in clusters of Zr_mC_n implies that rather than the formation of cubic structures, a multi-growth mechanism is operative and responsible for the magic numbers of metallocarbohedrenes. Hence, while it might be suggested that a cubic structure with eight metals at the corners and twelve carbons connecting in-between could possibly explain the predominant peaks observed at (8,12), such an explanation is not compatible with the growth mechanism of the Met-Cars. Although several alternative growth mechanisms have been proposed, [8,9,58] they are still in debate and await additional experimental attention.

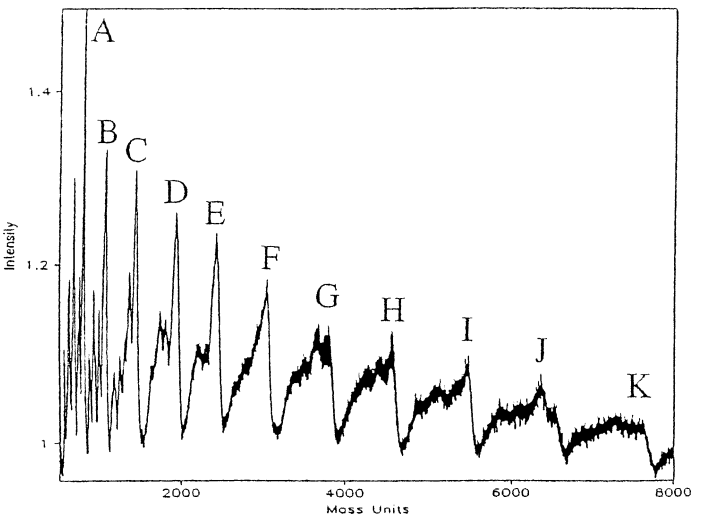

Figure 5. Mass spectra of the photoionized neutral $(TiN)_n$ clusters. Note the mass spectral abundance patterns indicate that the clusters have cubic-like structures resembling pieces of the fcc lattice of solid TiN. (A) $Ti_{14}N_{13}$ [3 × 3 × 3], (B) $Ti_{18}N_{18}$ [4 × 3 × 3], (C) $Ti_{24}N_{24}$ [4 × 4 × 3], (D) $Ti_{32}N_{32}$ [4 × 4 × 4], (E) $Ti_{40}N_{40}$ [5 × 4 × 4], (F) $Ti_{50}N_{50}$ [5 × 5 × 4], (G) $Ti_{63}N_{62}$ [5 × 5 × 5], (H) $Ti_{75}N_{75}$ [6 × 5 × 5], (I) $Ti_{90}N_{90}$ [6 × 6 × 5], (J) $Ti_{108}N_{108}$ [6 × 6 × 6], (K) $Ti_{126}N_{126}$ [7 × 6 × 6].

5. Structural considerations and reactions

Although a T_h structure was found to be most consistent with the experimental findings, a number of theories now suggest a structure with T_d symmetry, composed of a tetracapped tetrahedral metal skeleton, as originally proposed by Dance [38]. The major difference between the originally proposed pentagonal dodecahedron of T_h symmetry and the aforementioned T_d structure lies in the number of distinct metal sites on the surface of the cluster. For the T_h structure, each metal site in the cluster occupies an identical position leading to only one type of metal environment; however, there are two distinct positions for the metal sites in the tetracapped tetrahedron structure, four each in the inner tetrahedron, and four in the outer tetrahedron. These sites are distinguishable by various preferred coordination numbers. Ligand titration experiments, however, generally support T_h symmetry. Subsequent titration studies were conducted with larger ligands that would be expected to display steric effects. Experiments with 2-butanol, which is much larger than water and ammonia thus giving rise to steric effects upon attachment to those two sets of metal atoms, were conducted with titanium Met-Cars. The product distribution of $Ti_8C_{12}^+$ with 2-butanol showed no preference for the attachment of four molecules, and the product intensity was found to smoothly continue until truncation at $Ti_8C_{12}^+(2\text{-butanol})_8$ [59].

Other studies with π-bonding molecules (acetonitrile and pyridine, for example) were observed to terminate at $Ti_8C_{12}^+(\pi\text{-bonding molecules})_4$ [59]. The arrangement of these four π-bonding molecules may correspond to the attachment onto the faces through bridging to two metal atoms of the tetrahedron of the T_d structure. As discussed later in this review, other data and theoretical findings strongly support a T_d structure.

Another interesting finding during the course of the titration experiments was the apparent loss of one carbon atom from some of the structures comprised of M_8C_{13} when eight ligands were bonded. This led to the formation of $(M_8C_{12})L_8$, where L represents the ligand. Significantly, depending on the conditions of formation, a portion of the M_8C_{13} distribution retained the extra carbon atom even with the uptake of eight ligands, strongly pointing to these species being Met-Cars with an endohedral carbon atom [60].

Additional investigations made in our laboratory also revealed some surprising reaction behavior in that for the case of acetone, $Ti_8C_{12}^+$ is found to mainly undergo an association reaction, while the $Ti_7NbC_{12}^+$ and $Nb_8C_{12}^+$ species undergo a reaction that leads to the extraction of one and two oxygen atoms, respectively [61]. These products can thereafter undergo sequential clustering with acetone and it was determined that the mechanism involves the breaking of the carbonyl bond and subsequently forming M–O bonds due to the presence of a charged Nb atom. Other interesting reactions have also been observed with

methyl halides and it was found that methyl iodide undergoes abstraction reactions with titanium, niobium, and mixed titanium Met-Cars through insertion into the C–I bond. A second channel, only observed with the niobium-containing species, is the abstraction of a methyl group, which is not found for the Ti_8C_{12} [61]. The unusual selective chemistry of these species prompts interest in pursuing further studies of their reactive behavior [62].

6. Ionization of Met-Cars

6.1. Determination of ionization potentials

Ionization potentials (IPs), as well as electron affinities, are parameters which are experimentally measurable and theoretically calculable, thus enabling a comparison of predictions and experiments. The findings are also valuable in giving some additional insights into structure. For Met-Cars, many theoretical studies have predicted the IPs for different geometric structures based on the density functional method of various levels. Table 3 summarizes the IPs for Met-Cars of several metals for two proposed geometric structures [25,29,31,63,64], namely, a pentagonal dodecahedral cage structure with T_h symmetry and a tetracapped tetrahedron with T_d symmetry [38]. It is seen in Table 3 that the IPs for the T_d structure are calculated to be lower than those for the T_h structure for Met-Cars of the same metal element. This suggests that, despite the uncertain accuracy of deducing absolute IPs through density functional calculations, progress may be made toward answering the controversy about the geometric structure of the Met-Cars by experimentally determining their IPs.

The photoionization efficiency (PIE) spectra for the titanium and zirconium Met-Cars near threshold are shown in Fig. 6. The sharp onset in Fig. 6, for single photon absorption, corresponds to the ionization threshold of each Met-Car. Because the PIE spectra are well fitted by straight lines, as shown in Fig. 6, the linear extrapolation method was adopted to deduce the IPs, and they were determined to be 4.40 ± 0.02 and 3.95 ± 0.02 eV for the titanium and zirconium Met-Cars, respectively [43]. The PIE of the titanium-

Table 3. Ionization Potentials (eV) for the titanium, vanadium, zirconium, and niobium Met-Cars.

Symmetry	Ti_8C_{12}	V_8C_{12}	Zr_8C_{12}	Nb_8C_{12}	Reference
			Theoretical calculations		
T_h	6.05				[25]
	5.33	5.92	4.89		[29]
	5.92				[31]
T_d	4.5				[60]
	4.37	5.53	3.99		[60]
	4.7[b]/4.60[c]	5.5[b]	4.2[b]/4.10[c]	5.4[b]	[61]
			Experimental measurements		
	4.9	>5.76	>5.76	>5.76	[60]
	4.4		3.95		[43]

[a] All theoretical values were obtained by density functional calculations of various levels. Unless noted, theoretically calculated IPs are not specified to be either vertical or adiabatic in the references.
[b] Vertical IPs.
[c] Adiabatic IPs.

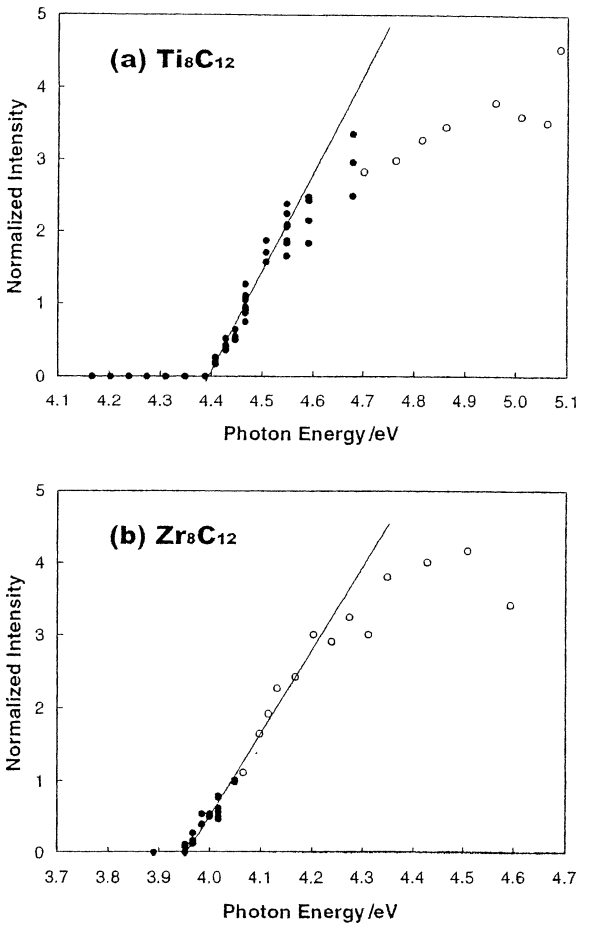

Figure 6. PIE plots for the pure titanium and zirconium Met-Cars.

zirconium mixed Met-Cars of the stoichiometry $Ti_{8-x}Zr_xC_{12}$ ($x = 1$–4) were also investigated, and their IPs are plotted in Fig. 7, along with those of the pure metal Met-Cars. Intriguingly, the IP decreases continually as the number of substituting zirconium atoms increases. This is surprising in view of the IPs of the constituent atoms being nearly the same (titanium: 6.82 eV and zirconium: 6.84 eV), and even more surprising, is the low IP values measured in light of the fact that the IP of carbon is 11.26 eV.

Through extensive investigations under widely varying conditions, we have found that it is critical that the Met-Cars are fully dehydrogenated to obtain an accurate ionization potential measurement. As seen in Fig. 7, the ionization potential of the pure Ti Met-Car drops upon substitution of Zr for Ti in the cluster and begins to approach the ionization potential of the pure Zr Met-Car. The measured values [43] agree well with values obtained via high-level density functional calculations [44].

An important question regarding ionization potential measurements of gas phase clusters is whether the clusters are warm enough to cause an artificially low ionization potential measurement. Subsequent experiments were conducted employing an additional cooling method in conjunction with the cluster source. Importantly, no difference in the values of the ionization potentials was observed, confirming the original measurements. Also, as the Met-Car clusters were cooled a significant observation was made. Up to four intact methane molecules were observed to cluster to the neutral Met-Car species [65]. Not only does this provide confirming evidence for the existence and stability of the neutral Met-Cars, it also establishes that the clusters exiting the source are very cold. The addition of methane molecules to the Met-

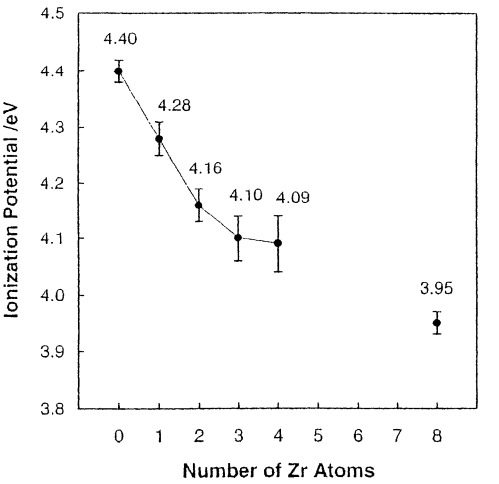

Figure 7. Ionization potentials for the $Ti_{8-x}Zr_xC_{12}$ ($x = 0{-}4, 8$) clusters.

Car clusters was observed to cause a small decrease in their ionization potentials, see Table 3. This effect is also in accord with observed effects on metal surfaces, where the work function of a metal can be lowered by the absorption of certain types of molecules.

These experimentally determined IPs are compared with the theoretically predicted IPs listed in Table 3. For both the titanium and the zirconium Met-Cars, the measured IPs agree quite well with the IPs which were calculated for the geometry with the T_d symmetry imposed. Therefore, if we assume high accuracy in the density functional calculations to estimate the IPs, this good agreement suggests that the Met-Cars have the geometry with T_d symmetry. In addition, the calculations have shown that the total energy of the T_d structure is lower than the total energy of the T_h structure [44].

In addition to the numerous experiments conducted on neutral and cationic Met-Car clusters, many negative ion studies have been preformed as well [66,67]. Most of these experiments have utilized anion photoelectron spectroscopy (PES) and have proved quite beneficial in revealing some of the intriguing electronic structure that these clusters possess. Wang and coworkers, for example, have investigated a variety of Met-Car species and have found that a surprisingly low electron affinity is very common among this class of clusters. Also, the recorded PES spectra seem to further point at the structure being of T_d symmetry, as did the IP studies, in that there are limited discrepancies when interpreting spectra in comparison to the molecular orbital schemes. The adiabatic electron affinity of the titanium Met-Car was measured at 1.05 eV, and 1.80 eV for the vanadium Met-Car [67].

7. Dynamics of Met-Car excitation and ionization

7.1. Delayed ionization and considerations of thermionic emission

The phenomenon of delayed ionization in clusters has been reported for several systems including the Met-Cars [68–70], pure transition metals [71–73], metal oxides [74–76], metal carbides [76], and the fullerenes [77–79]. Currently there is extensive interest in the origin of this phenomenon, prompting extensive theoretical and experimental investigations for various systems. In order for a cluster to display delayed ionization in a manner analogous to bulk phase thermionic emission, two important criteria must be fulfilled: (1) the ionization potential of the cluster must be less than its dissociation energy; and (2) all of phase space must be accessed by the system. The first requirement ensures that ionization, as an energy dissipation mechanism, will be more favorable than dissociation. Theoretical calculations and experimental results show that Met-Car clusters meet this requirement. The second requirement enables the system to temporarily store energy in excess of the cluster's ionization potential through statistically sampling a large number of accessible vibrational and electronic states.

Studies of Met-Cars employing time-of-flight mass spectrometry have often shown that the resolution was much lower than what was instrumentally achievable using the same apparatus to studying other systems. This observation, coupled with the fact that previous results suggested that the Met-Car clusters could be easily ionized with almost any laser wavelength, prompted us to undertake a detailed investigation of the ionization dynamics of this system.

Studies conducted in our laboratory employing nanosecond lasers revealed that some degree of ionization occurred on a time scale orders of magnitude longer than what is characteristic of normal photoionization obeying the photoelectric effect. In order for the delayed ionization to be observed for Met-Cars, the clusters must have some way to accommodate the energy necessary for the ionization to occur, while at the same time not undergo dissociation into smaller cluster fragments. Metallocarbohedrenes are thus ideal systems to exhibit this behavior, because when comparing the experimentally measured ionization potential (IP) and the theoretically predicted value for the dissociation energy (E_{diss}), a favorable relationship ($IP/E_{diss} < 1$) exists for this family of cluster molecules. This favorable relationship and the large density of electronic states for these transition metals–carbon species, may allow for the clusters to 'store' the energy gained during the excitation and delay ionize on the observable time scale of the experiment.

In the case of titanium–carbon clusters, delayed ionization was observed only for Met-Cars, and not for the rest of the metal–carbon cluster distribution [70]. At high laser fluences, above approximately 50 mJ/cm^2, a second delayed channel which corresponds to an atomic ion emission was observed [68,69]. Neither of these delayed ion channels, however, exhibit a dependence on the laser excitation wavelengths of 532 and 355 nm, but each channel did display a strong dependence on the fluence of the excitation laser. Similar findings have been consistently seen in all of the Met-Car systems studied, including Ti_8C_{12}, V_8C_{12}, Zr_8C_{12}, as well as the binary metal containing Met-Cars $Ti_xZr_yC_{12}$ and $Ti_xNb_yC_{12}$ (where $x + y = 8$). Further, a delayed atomic ion emission channel has been observed only for the Ti^+ component in the binary metal Met-Car systems. Clearly, Met-Car clusters do possess interesting electronic properties that may be controllable through the inclusion of various 'dopant' metals into the cagelike structural motif [69].

Even in those metal–carbon systems that display delayed ionization for clusters other than those of the Met-Car stoichiometry, in all of the pure metal systems investigated (Ti, Zr, Nb), the cluster corresponding to the Met-Car stoichiometry was found to be the dominant delayed species at all wavelengths investigated [70]. It should be noted that for single metal Met-Cars, the rate of delayed ionization is dependent on the type of metal incorporated into the cluster, while in the mixed metal Met-Cars, a non-monotonic dependence was found with respect to the degree of metal substitution [69].

Further extensive studies of the phenomenon revealed that delayed ionization is strongly dependent on the photoionization fluence, and at moderately low fluences the delayed ion yield has been found to approach 70% of the total Met-Car yield in the case of titanium, and similarly high in other systems as well [69]. The phenomenon has also been found to be present over a wide range of the spectral region, providing evidence that excitation to a specific (e.g., triplet) state is not responsible for the observed delayed ionization [70]. The general process of delayed ionization can be considered in the context of the Richardson–Dushman equation of the analogous bulk phenomenon. This equation has been reformulated by Klots to take into account the finite size of the system and the collection of excited species having a distribution of internal energies [80]. When compared to Klots' theory, the data for the mixed metal Met-Cars show a non-monotonic behavior with respect to metal substitution, and that it is found to correlate well with the ionization potential/work functions also measured in our laboratory; see Table 3 and Fig. 7.

The assumptions made in the statistical approach employed to model the experimental findings are that energy randomization occurs on the nanosecond timescale after laser excitation and the clusters do not dissociate. Although the model does not include other possible cooling mechanisms, good agreement is achieved between the statistical model of Klots and the experimental data. Taken together, the aforementioned observations generally support the thermionic emission model, which assumes that the energy deposited in the cluster is distributed over all accessible electronic states and there is not a specific long-lived state involved.

In order to shed further insight into the role of thermionic emission in the observed delay ionization behavior, we consider the approach of Klots [80] in more detail, employing a general procedure employed by Leisner et al. [71]. Upon irradiation of the ionization laser, Met-Cars absorb several photons where the number m depends on the laser fluence and the photoabsorption cross-sections of the Met-Cars. If we assume a Poisson distribution for the probability of photoabsorption, the probability that Met-Cars absorb m photons is given as

$$\rho(m,\overline{m}) = \frac{(\overline{m})^m}{m!}\exp(-\overline{m}) \tag{1}$$

where $\overline{m} = I\sigma/h\nu$ and is defined as the mean number of absorbed photons, I is the laser power density [J·cm^{-2}], σ is the photoabsorption cross section of the Met-Car [cm^2], and $h\nu$ is the photon energy of the laser [J]. Under a typical experimental condition where $I = 0.080$ J·cm^{-2} and $h\nu = 5.6\times10^{-19}$ J (355 nm), $\overline{m}$ is calculated to be approximately 1.4 assuming the cross section as $\sigma = 2.0\times10^{-16}$ cm^2. (That is, some Met-Cars absorb only a single proton, while others absorb two or more photons.) Using ρ, the number of neutral Met-Cars at $t = 0$ which adsorbed m photons, $N_0(m)$, is given as

$$N_0(m) = N_0\rho(m,\overline{m}) \tag{2}$$

where N_0 is the number of the neutral Met-Cars initially in a volume which interacted with the radiation from the ionization laser.

The difference in the number of absorbed photons causes different internal energies in the Met-Cars and hence different thermionic emission rates. If we focus solely on Met-Cars of a certain metal composition (i.e., they all possess the same ionization potential and heat capacity) and assume the internal energy for all of the Met-Cars before the photoexcitation is the same, the electron emission rate constants, k (as defined by Klots), depend uniquely on the number of the absorbed photons m. The ionization (electron emission) rate is assumed to be proportional to the number of excited neutral Met-Cars, and then the number of delayed ions produced between $t = 0$ and t after absorbing m photons, $N_0^t(m)$ is given as

$$N_0^t(m) = N_0(m)\bigl\{1 - \exp\bigl[-k(m)t\bigr]\bigr\} \tag{3}$$

where $k(m)$ is the electron emission rate constant after absorbing m photons. Finally, using Eqs. (1)–(3), the overall number of the delayed Met-Car ions formed between $t = t_1$ and t_2, which was measured in the experiment, is given as

$$\begin{aligned} N_{t_1}^{t_2} &= \sum_m \bigl\{N_0^{t_2}(m) - N_0^{t_1}(m)\bigr\} \\ &= N_0\sum_m \rho(m,\overline{m})\bigl\{\exp\bigl[-k(m)t_1\bigr] - \exp\bigl[-k(m)t_2\bigr]\bigr\} \end{aligned} \tag{4}$$

Since our experimental data did not provide absolute numbers of the delayed ions, both experimental data and theoretical values obtained from equation (4) were normalized such that the intensity at $t_1 = 0.10$ μs (or 0.15 μs) was unity when plotted together versus t_1. The fitting of the theoretical curve to the experimental data points was accomplished by setting the ionization potentials (when unknown), photoabsorption cross sections, and initial internal energies as variable parameters. Because of the normalization, the fitting was only qualitative; best fits were obtained by adjusting the parameters such that the shape of the model curve most closely resembled the temporal behavior of the experimental data points. These investigations were conducted on Met-Cars of various metal compositions (hence of various electronic structure) and by employing different photoexcitation wavelengths, based on the idea that, if the delayed ionization of the Met-Cars is truly 'thermionic', similar time evolution patterns should be observed for the various Met-Car species. Klots' formalism for the treatment of electron emission from small particles was used to model

the experimental results shown in Figs. 8a and 8b, which present findings for the zirconium and niobium systems [81]. In order to determine a reasonable value for the metal cluster temperature used in the modeling procedure, we performed a series of variable temperature experiments similar to the ones used to ensure the clusters were cold in the IP study [65]. The major adjustable parameter left in the modeling procedure is the ionization potential and the best agreement between the model and experiment always corresponded well with the experimentally measured ionization potentials.

It also was found that the delayed ionization model predicted the experimental trends observed with changing excitation wavelength, as is seen in Fig. 9 for the zirconium Met-Car system. The experimental findings, in comparison with the theoretical modeling, tend to support the thermionic emission model, and indicate that all of phase space may be sampled following their excitation over a range of wavelengths [70,81].

By studying the thermionic emission model and Eq. (4) carefully, it is found that the delayed ionization fitting curves gives almost identical shapes under different parameter settings. As an example, using the same initial temperature and cross section, the temporal evolution for the zirconium and niobium Met-Cars in Fig. 8 are well fitted, even when the IPs were set at 3.15 and 4.45 eV, respectively [70]. This is a consequence of the fact that when high IP values are employed, the processes for $m = 4$ (Zr) and $m = 5$ (Nb) have electron emission rates of about $10^6 - 10^7$ s^{-1} and dominate the curve shapes, while the processes for $m = 3$ (Zr) and $m = 4$ (Nb) dominate the curve shapes when the lower IPs are assumed. Therefore, finding IP values which give good-fitting curves, with other parameters fixed, does not guarantee a unique determination of the actual IP values.

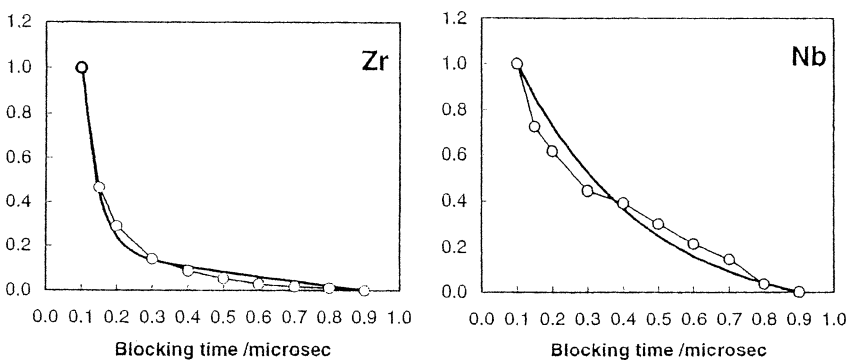

(a) (b)

Figure 8. Plots of experimental data for (a) Zr_8C_{12}, (b) Nb_8C_{12}. Neutral Met-Car species photoionized at 355 nm, and the solid curves are calculated using the thermionic emission model.

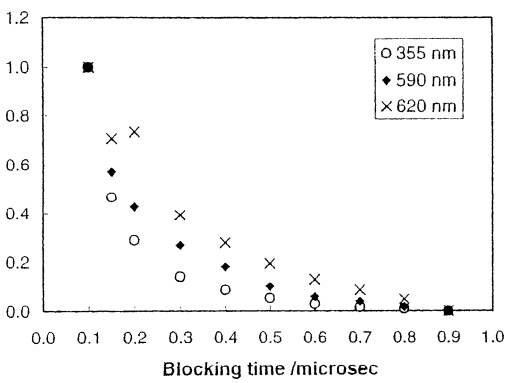

Figure 9. Delayed ionization behavior of Zr_8C_{12} as a function of the wavelength of the ionization laser: 355, 590, and 620 nm.

Regarding the temperature of the clusters, the absolute value may not be meaningful because we do not know the absolute heat capacities of Met-Car clusters and their dependence on temperature. It is assumed in our analyses that the heat capacity of a cluster composed of n atoms is given as $(3n - 6)kT$ at any temperature, but this may not be a good assumption at low temperatures when some of the vibrational modes in the cluster are inactive, and thus do not effectively serve to store energy. Therefore, without the knowledge of the heat capacity, we cannot evaluate whether the assumed temperature, e.g., 100 K, is physically reasonable and even comparable with those obtained under other experimental methods. As for the photoabsorption cross section, it may not be appropriate to assume that the cross section is equal for different Met-Cars and at different wavelengths, although the effect of the cross section on the curve shape is not always significant. In any case, these results suggest that additional information on the parameters must be obtained to further understand the delayed ionization behavior for the different species observed under the different experimental conditions. Indeed, whether true thermionic emission is actually the operative mechanism at the molecular level is currently in question and represents a subject of substantial current interest.

7.2. Ionization via reaction

A novel physical and chemical phenomenon has been discovered in the process of studying the oxidation of Met-Cars: the oxidation induced formation of $Ti_8C_{12}^+$ [82]. Experiments were conducted by interacting neutral titanium–carbon species from the laser-induced plasma source with O_2 after totally excluding cluster ions from the beam by a mass filter and ion optics. The selective formation of only $Ti_8C_{12}^+$ was observable when neutral species emanating from the plasma reactor were interacted with O_2, although several other reactants, including Cl_2 and N_2O, were also employed under identical experimental conditions with no resulting ion products being found. These results show that the present chemical process is not common chemi-ionization. Although the exact neutral precursors are unknown, this process is closely related to the facts that: (1) Ti_8C_{12} is a stable cluster molecule; and (2) Ti_8C_{12} has an unusually low ionization potential of about 4.4 eV. Although we cannot detect the other products of reaction, they may be CO and/or TiO, which could be responsible for this being a highly exothermic oxidation process. In comparison with other experimental results, the first step of this process is speculated to result from the formation of CO molecules, in which the released energy heats the Met-Car cluster to highly excited electronic states. The process can be represented as follows:

$$\mathrm{Ti}_{8+x}\mathrm{C}_{12+y} + n\mathrm{O}_2 \rightarrow \mathrm{Ti}_8\mathrm{C}_{12}^* + y\mathrm{CO} \quad \text{and/or} \quad x\mathrm{TiO} \tag{5}$$

where * denotes a highly excited species. There are two ways for these highly excited Met-Cars to lose one electron; through electron transfer to O_2 molecules and by thermionic emission. A search for negative O_2 ions did not reveal any anions, and thus the operative mechanism for the formation of $Ti_8C_{12}^+$ apparently occurs through thermionic emission.

8. Femtosecond spectroscopy: the dynamics of cluster excitation

Since the discovery of Met-Car clusters, and especially the observation of their low ionization potentials and delayed ionization phenomena, there has been interest in determining dynamical aspects of their electronic properties. Although Met-Cars have attracted considerable interest from the theoretical community, many details concerning the electronic structure of the Met-Car clusters are not well known due to the complexity associated with calculations on systems with numerous electrons. Understanding the basic phenomenon associated with the excitation and relaxation dynamics of systems of finite size is a subject of extensive current interest as it relates to the evolving electronic band of states of nanoscale materials and their properties.

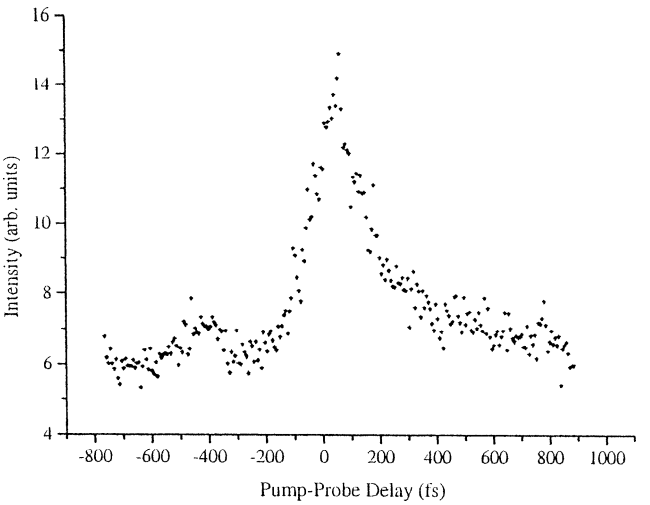

Figure 10. 620/400 nm pump-probe transient observed for vanadium Met-Car.

The most promising method to study these phenomena is through the use of ultrafast laser pump-probe techniques [83]. Regarding metal containing clusters, to date most studies have focused mainly on small systems such as alkali metal dimers [84,85] and trimers [86]. We have recently expanded our work to an investigation of metal–carbon complexes of much larger size, as well as to other non-metal systems.

One valuable series of experiments were performed in our laboratory on the excited state dynamics of various vanadium–carbon clusters employing the pump-probe technique [87]. Particular emphasis has been placed on elucidating laser fluence effects on such clusters, as well as the role of varying the wavelengths employed. In addition to determining the time-resolved measurements of electronic relaxation in various vanadium–carbon clusters, including the vanadium Met-Car, data revealing nuclear vibrational motion has been extracted as well.

The ultrafast dynamics of vanadium–carbon clusters were investigated under 400 nm pump, 620 nm probe conditions and similarly at wavelengths of 800 nm and ∼1200 nm [88]. In the case of the experimental trace shown in Fig. 10, the cross-correlation of the 400 nm pump and 620 nm probe beams was measured to be $\leqslant$ 86 fs while the pump-probe response of the V_8C_{12} cluster is 225 fs (FWHM). This measurable difference indicates that a state (or band of states) with an appreciable lifetime is being accessed and the corresponding fitted transients for a series of vanadium–carbon clusters, including V_8C_{12}, is illustrated in Fig. 11. The Met-Car response is noticeably longer than the autocorrelation width and since these clusters are strongly bound [50], the pump-probe response is likely too short to be attributable to a fragmentation process, either in the Met-Car cluster, or leading to the fragmentation of a larger cluster to form the Met-Car. The pump-probe response is thus attributed to the temporal dependence of the electronic relaxation behavior of this system.

It should also be noted that the pump-probe transients for all of the observed vanadium–carbon clusters with more than four metal atoms show a similar pump-probe response with exponential decays on the order of a few hundred femtoseconds. It is likely that a common chromophore [89], present in clusters as small as the V_4C_x series and extending up through the Met-Car, is being accessed. In addition, the excited state lifetimes are observed to narrow as the cluster size increases. This result suggests that the larger nanoscale complexes have more free-electron character and therefore the rate of energy relaxation is higher in the larger clusters. The long-time tail in the Met-Car spectrum suggests relaxation into a state or band of states.

Similar relaxation behavior is also observed at other wavelengths. For example, a typical pump-probe transient of the vanadium Met-Car at moderate laser fluence with photons of 800 nm and 1250 nm, is shown in Fig. 12. These findings begin to uncover the complexity of the density of excited electronic states involved, and the concomitant relaxation dynamics. Observations indicate that small changes in the

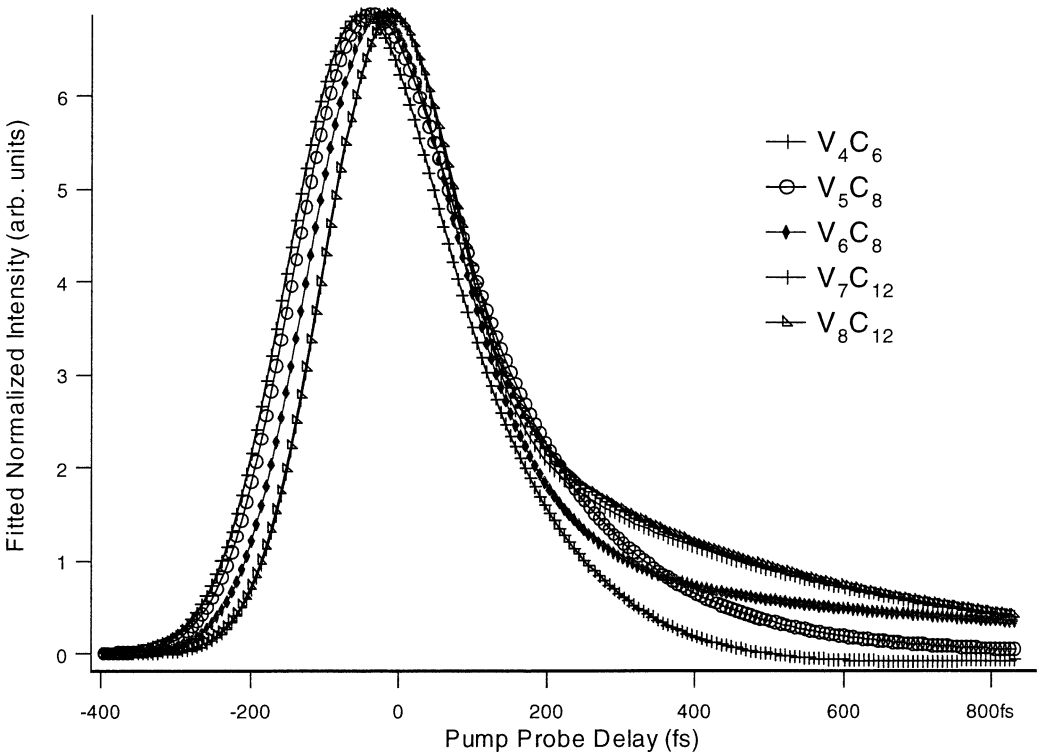

Figure 11. Summary of the fits of experimental pump-probe data for various vanadium–carbide clusters, including V_8C_{12}.

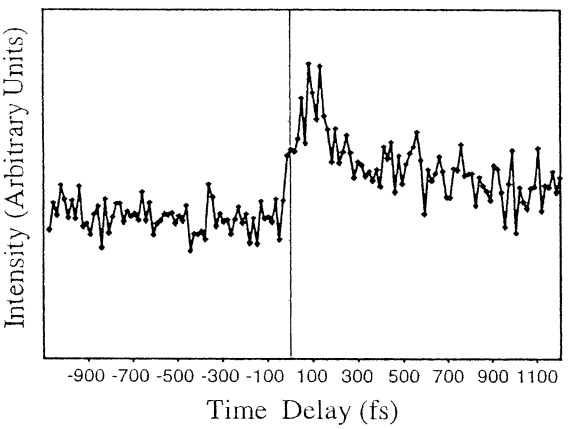

Figure 12. 1250/800 nm pump-probe transient observed for vanadium Met-Car.

1250 nm wavelength dramatically affect the behavior of the system pumped by the redder wavelength and probed and 800 nm. Clear evidence for electronic energy to lattice coupling modes has been acquired with findings that at long delay times the latter could contribute to the thermionic emission we have observed. Importantly, these new findings show that the delayed ionization process, typically seen only under excitation via nanosecond pulses, might be revealed in experiments conducted with laser fluences that enable relaxation into electronic bands during a femtosecond excitation process. This work is providing a new understanding of the process generally termed ‘thermionic’ ionization/emission, in terms of the

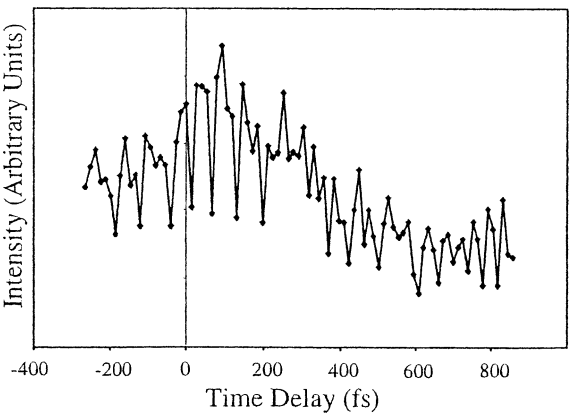

Figure 13. 1255/800 nm pump-probe transient observed for vanadium Met-Car. Note the oscillatory frequency: 505 cm^{-1}.

microscopic quantum effects that influence the dynamics of relaxation into electronic bands that govern the temporal characteristics of the phenomena.

Other recent investigations exploring the electronic excitation and relaxation properties of the vanadium Met-Car, using short unchirped pulses, have also enabled us to observe and characterize vibrational frequencies in the ionization dynamics; see Fig. 13. Periodic recurrences in the ionization intensities are readily seen, from which a frequency of 505 cm^{-1} is obtained [88]. Interestingly, this compares to a metal–carbon stretch frequency of 575 cm^{-1} reported for VC on vanadium surfaces [90]. Meijer and coworkers have extracted a similar vibration for Ti_8C_{12} with a frequency of 525 cm^{-1} [91].

9. The production of Met-Cars in the solid state

Pursuant to their discovery, we embarked on a study of methods to produce Met-Cars in the solid state [23,92]. The lack of any hydrogen component in the observed mass spectra of the $M_mC_n^+$ suggested that efficient dehydrogenation reactions take place in the plasma and the question still remains on how this process commences. Are the hydrocarbons cracked (subsequently losing hydrogen atoms in multiple collisions with energetic electrons or other plasma constituents), or are they efficiently dehydrogenated by reactions with the transition-metal atoms or ions present in the plasma? The first studies of the reaction mechanisms raised questions about the possible role of partially dehydrogenated hydrocarbons as intermediates in the formation of Met-Cars. Also, working out an efficient synthesis routine for producing bulk amounts of metallocarbohedrenes depends on knowledge of the mechanisms and knowing what form of carbon should be introduced into the reactor.

The result of a TOF-MS analysis of one sample of raw soot, either produced through the direct laser vaporization of pressed rods of various molar ratios or an arc discharge, is shown in Fig. 14. In order to confirm our successful production of Met-Cars, we also generated a soot sample from vanadium with similar success; see Fig. 15. The expected shift of 24 amu from 528 to 552 amu is evident, establishing the presence of the vanadium analog of V_8C_{12} in the sample. Moreover, we can assign the 540- and 564-amu species to V_8C_{11} and V_8C_{13}, respectively. These species are also observed in molecular beam studies of the vanadium derivatives of the Met-Car [92]. Additionally, the soot samples were found to be quite inhomogeneous and, not surprisingly, contained C_{60}, and to a lesser extent C_{70}. Consideration has also been given to their stability in air as well as through ligand attachment [92,93].

Being aware that laser desorption can generate a range of products depending on the sample, we conducted other experiments to confirm that we actually desorb Met-Cars in the analysis of the soot and do not produce them during analysis. Most importantly, it is highly unlikely that we would produce M_8C_{12} (M=Ti, V) molecules within the sample with one laser pulse and desorb them with subsequent pulses. The Met-Car signal is observed immediately (< 10 laser shots) and the signal intensity thereafter decreases with

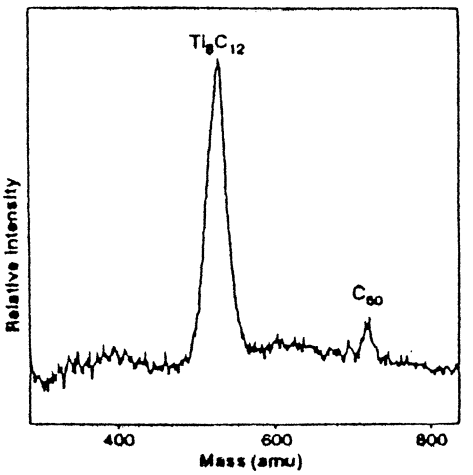

Figure 14. Laser desorption mass spectra of soot generated in an arc between two composite Ti–C electrodes (5 : 1 metal to carbon mass ratio). Ti_8C_{12}, and, to a lesser extent, C_{60}, are both present in the desorbed vapor.

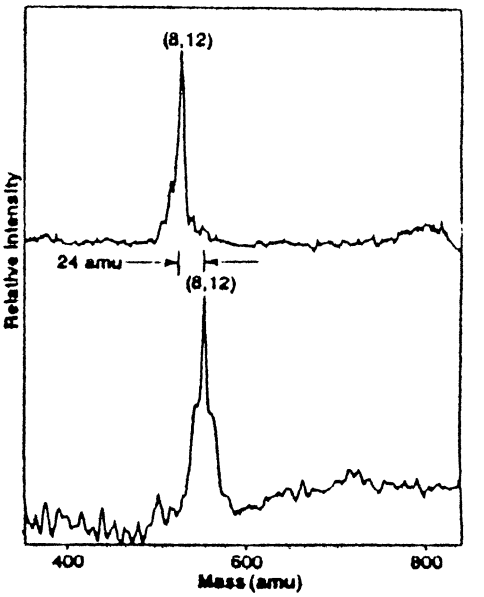

Figure 15. Mass spectra of laser desorption mass spectra of soot generated in a arc-discharge: top, Ti/C; bottom: V/C. Note the 24 amu shift between T_8C_{12} and V_8C_{12}.

time, neither of which would be expected if we produced Met-Cars in the soot sample with the desorption laser. Second, if the Met-Cars were generated during desorption via gas phase growth processes, we would expect to see their characteristic building pattern as is observed in the molecular beam experiments and in the mass distribution of the laser desorption experiments of pure graphite samples in which fullerenes are produced. We see no evidence of these processes occurring during desorption.

In light of being able to produce the Met-Cars via direct laser vaporization, we directed our attention, to the deposition of materials and study by STM [94]. An example of STM images of those species extracted with methanol from a zirconium-based soot sample, is illustrated in Fig. 16. These species, most likely the corresponding metal carbides, metal oxides, Met-Car clusters, and perhaps even pure metal clusters, were again generated via direct laser vaporization, and although a variety of species undoubtedly exist in the soot, zirconium oxides and similarly the carbides, are not very soluble in methanol, and thus are not likely present in the extraction. It should also be noted that since oxides are insulating materials, it is not likely that they will be imaged due to their inability to conduct electrons from the swinging STM tip.

In addition, the particles on the gold surface also appear as spherical protrusions of uniform size and it is again unlikely that the oxides and carbides would yield particles so symmetric given their known varied growth pattern. The cross sectional heights observed for the particles correlate with the expected diameter of 6 Å for the Met-Cars, and when coupled with some intriguing UV-Vis data, these findings further substantiate our preliminary assignment [94].

10. Conclusions

The discovery of a new molecular cluster system comprised of early transition metals bound in a 2 : 3 ratio with carbon was quite unexpected in view of the usual bonding of the transition metal carbides having a 1 : 1 stoichiometry. This aspect alone prompted considerable interest in these unique cluster species, further

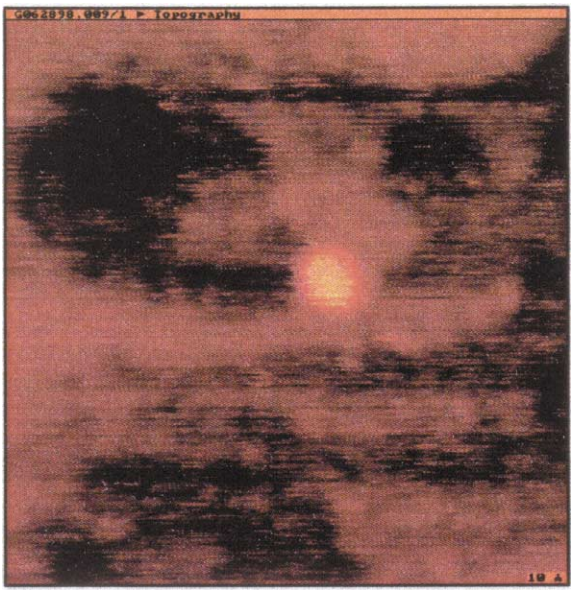

Figure 16. STM image of a particle from Zr-based Met-Car containing soot on MEA-modified Au{111}. Image size: 60 Å × 60 Å sample bias voltage: +400 mV, tunneling current: 1.0 nA.

stimulated by questions about their structure, mechanisms of formation, and the evolving distributions leading to the development of larger cage structures. Evidence that the assembly of eight MC_2 units, followed by the metastable loss of C_3 and C units as a mechanism of Met-Car formation, was also unique to these species. Met-Cars also undergo a variety of chemical reactions, attesting to and giving rise to interest in their rich chemistry.

Perhaps of most significance are the various electronic characteristics which we have uncovered, including their unexpectedly low ionization potentials, extensive fraction of delayed ionization, and observed unique mechanism of delayed atomic ion emission. These characteristics of Met-Cars have stimulated further interest in these species as potential new electronic materials. Though this aspect still awaits fruition, Met-Cars are recognized as unique caged clusters for studying strongly bonded systems where quantum confinement plays an important role in governing their properties. New findings, particularly ones arising from the use of different methods to study the underlying molecular details of delayed ionization, including femtosecond lasers and pump-probe experiments to investigate the deposition of energy into various electronic bands and subsequent relaxation processes, can be expected to give considerable new insight into the properties of Met-Cars and other clusters that may be promising systems for tailoring the design of nanoscale materials.

Acknowledgements. We gratefully acknowledge financial support by Air Force Office of Scientific Research Grants F49620-97-1-0183 and F49620-98-1-0406 (AASERT98) and Grant F49620-99-1-0099 from the Defense University Research Instrumentation Program (DURIP).

References

[1] B.C. Guo, A.W. Castleman Jr., J. Am. Soc. Mass Spectrom. 3 (1992) 464.
[2] B.C. Guo, A.W. Castleman Jr., Int. J. Mass Spectrom. Ion Proc. 113 (1992) R1.
[3] B.C. Guo, K.P. Kerns, A.W. Castleman Jr., Int. J. Mass Spectrom. Ion Proc. 117 (1992) 129.
[4] B.C. Guo, K.P. Kerns, A.W. Castleman Jr., J. Phys. Chem. 96 (1992) 6931.
[5] B.C. Guo, A.W. Castleman Jr., J. Am. Chem. Soc. 114 (1992) 6152.
[6] B.C. Guo, K.P. Kerns, A.W. Castleman Jr., Science 255 (1992) 1411.
[7] B.C. Guo, S. Wei, J. Purnell, S. Buzza, A.W. Castleman Jr., Science 256 (1992) 515.
[8] S. Wei, B.C. Guo, J. Purnell, S. Buzza, A.W. Castleman Jr., J. Phys. Chem. 96 (1992) 4166.
[9] S. Wei, B.C. Guo, J. Purnell, S. Buzza, A.W. Castleman Jr., Science 256 (1992) 818.

[10] B.C. Guo, S. Wei, Z. Chen, J. Purnell, S. Buzza, K.P. Kerns, A.W. Castleman Jr., J. Chem. Phys. 97 (1992) 5243.
[11] Z.Y. Chen, B.C. Guo, B.D. May, S. Cartier, A.W. Castleman Jr., Chem. Phys. Lett. 198 (1992) 118.
[12] A.W. Castleman Jr., B.C. Guo, S. Wei, in: V. Kumas, T.P. Martin, E. Tosatti (Eds.), Clusters and Fullerenes, World Scientific, Singapore, 1993, p. 3.
[13] A.W. Castleman Jr., B.C. Guo, S. Wei, Z.Y. Chen, in: K. Lackner, W. Lindinger (Eds.), Plasma Physics and Controlled Fusion, Vol. 34, Pergamon Press, Oxford, 1992, p. 2047.
[14] B.C. Guo, A.W. Castleman Jr., in: M.A. Duncan (Ed.), Advances in Metal and Semiconductor Clusters, Vol. 2, JAI Press, 1994, p. 137.
[15] A.W. Castleman Jr., 1994 McGraw-Hill Yearbook of Science and Technology, 1993, p. 263.
[16] A.W. Castleman Jr., Z. Phys. D. 26 (1993) 159.
[17] Z.Y. Chen, A.W. Castleman Jr., in: Proc. 40th ASMS Conference on Mass Spectrometry and Allied Topics, 1992, p. 1480.
[18] A.W. Castleman Jr., R&D Innovator 2 (February 1993).
[19] B.C. Guo, K.P. Kerns, A.W. Castleman Jr., J. Am. Chem. Soc. 115 (1993) 7415.
[20] Z.Y. Chen, G.J. Walder, A.W. Castleman Jr., Phys. Rev. B 49 (1994) 2739.
[21] Z.Y. Chen, A.W. Castleman Jr., J. Chem. Phys. 98 (1993) 231.
[22] B.C. Guo, K.P. Kerns, A.W. Castleman Jr., J. Chem. Phys. 96 (1992) 8177.
[23] Z.Y. Chen, G.J. Walder, A.W. Castleman Jr., J. Phys. Chem. 96 (1992) 9581.
[24] R.W. Grimes, J.D. Gale, J. Chem. Soc., Chem. Commun. (1992) 1222.
[25] B.V. Reddy, S.N. Khanna, P. Jena, Science 258 (1992) 1640.
[26] T. Rantala, D.A. Jelski, J.R. Bowser, X. Xia, T.F. George, Z. Phys. D. 26 (1993) 255.
[27] M. Methfessel, M. van Schilfgaarde, M. Scheffler, Phys. Rev. Lett. 70 (1993) 29.
[28] P. Jena, S.N. Khanna, B.K. Rao, in: V. Kumar, T.P. Martin, E. Tosatti (Eds.), Clusters and Fullerenes, World Scientific, 1992, p. 73.
[29] R.W. Grimes, J.D. Gale, J. Phys. Chem. 97 (1993) 4616.
[30] B.V. Reddy, S.N. Khanna, Chem. Phys. Lett. 209 (1993) 104.
[31] B.-L. Li, Z.-Q. Gu, R.-S. Han, Q.-Q. Zheng, Z. Phys. D. 27 (1993) 275.
[32] L. Lou, T. Guo, P. Nordlander, R.E. Smalley, J. Chem. Phys. 99 (1993) 5301.
[33] A. Ceulemans, P.W. Fowler, J. Chem. Soc. Faraday Trans. 88 (1992) 2797.
[34] L. Pauling, Proc. Natl. Acad. Sci. 89 (1992) 8175.
[35] M.-M. Rohmer, P. De Vaal, M. Bénard, J. Am. Chem. Soc. 114 (1992) 9696.
[36] Z. Lin, M.B. Hall, J. Am. Chem. Soc. 114 (1992) 10054.
[37] P.J. Hay, J. Phys. Chem. 97 (1993) 3081.
[38] I. Dance, J. Chem. Soc., Chem. Commun. (1992) 1779.
[39] H. Chen, M. Feyereisen, X.P. Long, G. Fitzgerald, Phys. Rev. Lett. 71 (1993) 1732.
[40] A. Khan, J. Phys. Chem. 97 (1993) 10937.
[41] M.-M. Rohmer, M. Bénard, C. Henriet, C. Bo, J.-M. Poblet, J. Chem. Soc., Chem. Commun. 15 (1993) 1182.
[42] Z. Lin, M.B. Hall, J. Am. Chem. Soc. 115 (1993) 11165.
[43] H. Sakurai, A.W. Castleman Jr., J. Phys. Chem. A 102 (1998) 10486.
[44] M.-M. Rohmer, M. Bénard, J.-M. Poblet, Chem. Rev. 100 (2000) 495.
[45] S.F. Cartier, B.D. May, A.W. Castleman Jr., J. Chem. Phys. 100 (1994) 5384.
[46] S.F. Cartier, B.D. May, A.W. Castleman Jr., J. Am. Chem. Soc. 116 (1994) 5295.
[47] H.T. Deng, B.C. Guo, K.P. Kerns, A.W. Castleman Jr., Int. J. Mass Spectrom. Ion Proc. 138 (1994) 275.
[48] J. Purnell, S. Wei, A.W. Castleman Jr., Chem. Phys. Lett. 229 (1994) 105.
[49] S. Wei, B.C. Guo, J. Purnell, S.A. Buzza, A.W. Castleman Jr., J. Phys. Chem. 97 (1993) 9559; Additions and Corrections, J. Phys Chem. 98 (1994) 9682.
[50] K.P. Kerns, B.C. Guo, H.T. Deng, A.W. Castleman Jr., J. Chem. Phys. 101 (1994) 8529.
[51] J.S. Pilgrim, M.A. Duncan, J. Am. Chem. Soc. 115 (1993) 4395.
[52] S. Wei, B.C. Guo, H.T. Deng, K.P. Kerns, J. Purnell, S.A. Buzza, A.W. Castleman Jr., J. Am. Chem. Soc. 116 (1994) 4475.
[53] J.S. Pilgrim, M.A. Duncan, J. Am. Chem. Soc. 115 (1993) 6958.
[54] J.S. Pilgrim, M.A. Duncan, J. Am. Chem. Soc. 115 (1993) 9724.
[55] J.S. Pilgrim, M.A. Duncan, Int. J. Mass Spectrom. Ion Proc. 138 (1994) 283.
[56] B.D. May, S.E. Kooi, B.J. Toleno, A.W. Castleman Jr., J. Chem. Phys. 106 (1997) 2231.
[57] S. Wei, A.W. Castleman Jr., Chem. Phys. Lett. 227 (1994) 305.
[58] L.-S. Wang, H. Cheng, Phys. Rev. Lett. 79 (1997) 2983.
[59] H.T. Deng, K.P. Kerns, A.W. Castleman Jr., J. Am. Chem. Soc. 118 (1996) 446.
[60] K.P. Kerns, B.C. Guo, H.T. Deng, A.W. Castleman Jr., J. Am. Chem. Soc. 117 (1995) 4026.

[61] H.T. Deng, B.C. Guo, K.P. Kerns, A.W. Castleman Jr., J. Phys. Chem. 98 (1994) 13373.
[62] Y.G. Byun, S.A. Lee, S.Z. Kan, B.S. Freiser, J. Phys. Chem. 100 (1996) 14281.
[63] L.R. Brock, M.A. Duncan, J. Phys. Chem. 100 (1996) 5654.
[64] J. Munoz, C. Pujol, C. Bo, J.M. Poblet, M.-M. Rohmer, M. Bénard, J. Phys. Chem. A 101 (1997) 8345.
[65] H. Sakurai, A.W. Castleman Jr., J. Chem. Phys. 111 (1999) 1462.
[66] L.-S. Wang, S. Li, H. Wu, J. Phys. Chem. 100 (1996) 19211.
[67] H. Li, H. Wu, L.-S. Wang, J. Am. Chem. Soc. 119 (1997) 7417.
[68] B.D. May, S.F. Cartier, A.W. Castleman Jr., Chem. Phys. Lett. 242 (1995) 265.
[69] S.F. Cartier, B.D. May, A.W. Castleman Jr., J. Chem. Phys. 104 (1996) 3423.
[70] S.E. Kooi, A.W. Castleman Jr., J. Chem. Phys. 108 (1998) 8864.
[71] T. Leisner, K. Athanassenas, O. Echt, D. Kreisle, E. Rechnagel, J. Chem. Phys. 99 (1993) 9670.
[72] T. Leisner, K. Athanassenas, O. Echt, O. Kandler, D. Kreisle, E. Rechnagel, Z. Phys. D 20 (1991) 127.
[73] B.A. Collings, A.H. Amrein, D.M. Rayner, P.A. Hackett, J. Chem. Phys. 99 (1993) 4174.
[74] B.C. Nieman, E.K. Parks, S.C. Richtsmeier, K. Liu, L.G. Pobo, S.L. Riley, High Temp. Sci. 22 (1986) 115.
[75] K. Athanassenas, T. Leisner, U. Frenzel, D. Kreisle, Ber. Bunsenges. Phys. Chem. 96 (1992) 1192.
[76] A. Amrein, R. Simpson, P. Hackett, J. Chem. Phys. 95 (1991) 1781.
[77] E.E.B. Campbell, G. Ulmer, I.V. Hertel, Phys. Rev. Lett. 67 (1991) 1986.
[78] D. Ding, J. Huang, R.N. Compton, C.E. Klots, R.E. Haufler, Phys. Rev. Lett. 73 (1994) 1084.
[79] H. Lin, K.-L. Han, Y. Bao, E.B. Gallogly, W.M. Jackson, J. Phys. Chem. 98 (1994) 12495.
[80] C.E. Klots, Chem. Phys. Lett. 186 (1991) 73.
[81] H. Sakurai, S.E. Kooi, A.W. Castleman Jr., J. Cluster Science 10 (1999) 493.
[82] H.T. Deng, K.P. Kerns, A.W. Castleman Jr., J. Chem. Phys. 104 (1996) 4862.
[83] A.H. Zewail, J. Phys. Chem. 100 (1996) 12701.
[84] S. Rutz, S. Greschik, E. Schreiber, L. Wöste, Chem. Phys. Lett. 257 (1996) 365.
[85] A. Assion, T. Baumert, J. Helbing, V. Seyfried, G. Gerber, Phys. Rev. A 55 (1997) 1899.
[86] S. Vajda, S. Rutz, J. Heufelder, P. Rosendo, H. Ruppe, P. Wetzel, L. Wöste, J. Phys. Chem. A 102 (1998) 4066.
[87] S.E. Kooi, B.D. Leskiw, A.W. Castleman Jr., Nano Lett. 1 (2001) 113.
[88] B.D. Leskiw, K.L. Knappenberger Jr., A.W. Castleman Jr., Relaxation dynamics of electronically excited vanadium–carbon clusters: excitation of the Met-Car, J. Chem. Phys., submitted.
[89] B. Bescós, B. Lang, J. Weiner, V. Weiss, E. Wiedenmann, G. Gerber, Eur. Phys. J. D 9 (1999) 399.
[90] B. Chen, J.G. Vries De, B.D. Frühberger, C.M. Kim, Z.-M. Liu, J. Vac. Sci. Technol. A 13 (1995) 1600.
[91] G. Heijnsbergen, D. Helden, M.A. Duncan, A.J.A. Roij, G. Meijer, Phys. Rev. Lett. 83 (1999) 4983.
[92] S.F. Cartier, Z.Y. Chen, G.J. Walder, C.R. Sleppy, A.W. Castleman Jr., Science 260 (1993) 195.
[93] R. Selvan, T. Pradeep, Chem. Phys. Lett. 309 (1999) 149.
[94] G.S. McCarty, J.C. Love, J.G. Kushmerick, L.F. Charles, C.D. Keating, B.J. Toleno, M.E. Lyn, A.W. Castleman Jr., M.J. Natan, P.S. Weiss, J. Nanoparticle Res. 1 (1999) 459.